Molecular simulation study on the solubility of Carbon Dioxide in mixtures of Cyclohexane + Cyclohexanone

T. Merker[a], J. Vrabec[b], H. Hasse[a,*]

[a] *Laboratory of Engineering Thermodynamics, University of Kaiserslautern, 67663 Kaiserslautern, Germany*
[b] *Thermodynamics and Energy Technology, University of Paderborn, 33098 Paderborn, Germany*

Abstract

Molecular simulation data on the vapor-liquid equilibrium and the Henry's law constant of carbon dioxide in mixtures of cyclohexane + cyclohexanone are presented. The agreement between simulation results and the available experimental data is good. For the present predictions, new molecular models for cyclohexane and cyclohexanone are developed. The resulting molecular models for cyclohexane and cyclohexanone show mean unsigned deviations with respect to experimental data considering the whole temperature range from triple point to critical point of 0.4 % and 0.9 % for the saturated liquid density, 3 % and 2.7 % for the vapor pressure, and 6 % and 5.3 % for the enthalpy of vaporization, respectively. The carbon dioxide model is taken from preceding work.

Keywords: cyclohexane, cyclohexanone, carbon dioxide, vapor-liquid equilibria, Henry's law constant, molecular simulation, Force field

1. Introduction

Molecular modeling and simulation is a modern approach for the prediction of thermophysical properties of pure fluids and mixtures, both in

*Corresponding author: Hans Hasse
Technische Universität Kaiserslautern, Lehrstuhl für Thermodynamik, Erwin-Schrödinger-Straße 44, 67663 Kaiserslautern, Germany, *phone* +49 631 205 3464, *fax* +49 631 205 3835
Email address: hans.hasse@mv.uni-kl.de (H. Hasse)
URL: thermo.mv.uni-kl.de (H. Hasse)

research and industry [1, 2, 3, 4, 5]. This is due to several reasons: Firstly, the predictive power of molecular models is superior to classical methods as it allows for accurate results for a wide range of states. Secondly, a given molecular model provides access to the full variety of thermophysical properties, such as structural, thermal, caloric, transport or phase equilibrium data. Finally, through the advent of cheaply available powerful computing infrastructure, reasonable execution times for molecular simulations can be achieved, which are crucial for industrial applications.

The oxidation of cyclohexane to cyclohexanol and cyclohexanone is an important industrial reaction and a key step in the nylon production chain. Usually, the reaction is carried out by contacting air with liquid cyclohexane at high temperature and high pressure [6]. Due to the formation of side products, the process must be carried out at a low conversion rate in order to allow for an acceptable selectivity towards cyclohexanone and cyclohexanol.

Therefore, alternative routes are being studied. One option are novel octahedral molecular sieves for the heterogeneously catalyzed selective oxidation of cyclohexane [7]. Liquids expanded by supercritical carbon dioxide can be used to enhance the mobility of both the reactants and the products, which is particularly important in such sieves. For a rational planning of the respective catalytic experiments and the process design, reliable thermodynamic data are needed. Such data, particularly at elevated pressures, are not available in the literature.

In this work, the Henry's law constant for carbon dioxide in liquid mixtures of cyclohexane + cyclohexanone was calculated by molecular simulation and compared to recently published experimental data from our group [8]. Therefore, new molecular models were developed for cyclohexane and cyclohexanone. For cyclohexane, a rigid six site Lennard-Jones (LJ) model and for cyclohexanone, a rigid seven site LJ plus point dipole model is proposed here.

The paper is structured as follows. Firstly, the new molecular models are presented, the corresponding pure substance vapor-liquid equilibria (VLE) and predictions of the second virial coefficient are compared to experimental data. Secondly, VLE simulations of the three binary mixtures containing carbon dioxide, cyclohexane and cyclohexanone are discussed and compared to experimental data. Thirdly, predictions of the Henry's law constant of carbon dioxide in liquid mixtures of cyclohexane + cyclohexanone are presented and compared to experimental data. Finally, the results are discussed and a conclusion is drawn.

2. Molecular Models

2.1. Carbon Dioxide

For carbon dioxide, a recently published molecular model [9] from our group was used. This model consists of three LJ sites and a quadrupole in its center of mass.

2.2. Cyclohexane

The molecular model for cyclohexane from preceding work of our group [10] was taken as a starting point here. The electrostatics of that model [10] was determined by quantum mechanical (QM) calculations resulting in a weak quadrupole moment of 0.8179 DÅ located in the center of mass. A detailed description of that calculation is given in [10]. Point quadrupole sites, located in the center of cyclic molecules, may lead to artefacts in molecular simulation [11]. Dividing the quadrupole equally into six parts and locating them at the six LJ sites representing the methylene (CH_2) groups, as done by Huang et al. [11] for benzene, leads to very small quadrupole magnitudes. Thus the polarity was neglected in the present cyclohexane model.

To optimize the model parameters to experimental VLE data, the method of Stoll [12] was employed, followed by the reduced unit method [13]. During both optimization steps, the size parameter of the LJ sites was slightly decreased (-0.2%) while the energy parameter was slightly increased (0.25%). The overall geometry was also sligthly scaled down (-0.16%). The cyclohexane model is sketched in Figure 1 and the parameters are given in Table 1.

Present VLE simulation results are shown in Figures 2 to 4 in comparison with experimental data, an equation of state (EOS) [14] and the model by Eckl et al. [10]. Despite the neglect of the quadrupole, no significant differences were found between the present model and the model by Eckl et al. [10]. The mean unsigned errors with respect to the EOS [14] for vapor pressure, saturated liquid density and enthalpy of vaporization are 1.7, 0.3 and 6 %, respectively, in the temperature range from 390 to 540 K, which is about 65 to 97 % of the critical temperature. The numerical simulation results and deviation plots are given in the supplementary material. The critical properties were determined through fits to the present VLE simulation results as suggested by Lotfi et al. [15]. Table 2 compares these critical properties to experimental data. The relative deviations between simulation

and experiment for the critical temperature and density are within 1 % and around 5 % for the critical vapor pressure.

To validate the predictive power of the cyclohexane model, simulations in the homogeneous region were performed and compared to the EOS [14] that was recommended by the National Institute of Standards and Technology, cf. Figures 5 and 6. 19 state points were studied, covering the liquid, supercritical and gaseous state. Relative deviations between simulation data and the EOS [14] for density and residual enthalpy are usually below 0.6 % and 3 %, respectively. The highest deviations for the density are in the supercritical region with a maximum of 11 %, whereas the highest deviations for the residual enthalpy are in the liquid region (around 3 %).

The second virial coefficient was predicted by evaluating Mayer's f-function as reported by Eckl et al. [10]. It is compared to the EOS [14] in Figure 7, where a good agreement can be seen throughout the entire regarded temperature range from 350 to 1000 K. The present numerical results are given in the supplementary material.

2.3. Cyclohexanone

A new molecular model for cyclohexanone was developed here based on QM calculations. It was optimized using experimental data on vapor pressure, saturated liquid density and enthalpy of vaporization employing the method of Stoll [12] and the reduced unit method [13]. As the complexity of a molecular model determines the computing time during molecular simulation, it was attempted to find an efficient solution balancing accuracy and simplicity. A rigid model with seven LJ sites and one point dipole was chosen. The internal degrees of freedom were neglected, as the cyclohexane ring predominantly assumes the energetically favorable chair conformation [16].

The geometry of the cyclohexanone model, i.e. bond lengths, angles and dihedrals, were directly passed on from QM calculations. The geometry optimization by energy minimization was carried out with GAMESS(US) [17]. The Hartree-Fock level of theory was applied with a relatively small (6-31G) basis set. One LJ site was located exactly at all resulting nuclei positions, except for the hydrogen atoms. The methylene group was modeled by a single LJ site, i.e. the united-atom approach was used. The coordinates of the seven LJ sites are given in Table 1 and a schematic of the molecular model is presented in Figure 1.

To describe the electrostatic interactions, one point dipole was placed at the arithmetic mean position between the carbon and the oxygen LJ site.

The point dipole is directed towards the oxygen atom. The coordinates and the orientation of the point dipole are given in Table 1.

A subset of the parameters for the LJ sites and the point dipole was optimized to the DIPPR correlations for saturated liquid density and vapor pressure of pure cyclohexanone [18] in the temperature range from 390 to 620 K. As a starting point for the optimization, the LJ parameters for the methylene site were taken from the cyclohexane model by Eckl et al. [10]. The remaining LJ parameters for the carbon and oxygen atoms were taken from a carbon dioxide model by Merker et al. [9]. The point dipole magnitude was taken from a carbon monoxide model by Stoll [12]. During the optimization, the LJ parameters of the methylene sites, the oxygen site and the point dipole magnitude were adjusted. The method of Stoll [12] was employed in the first step of this optimization. In the second step, the reduced unit method [13] was applied for a subsequent optimization. The final model parameters are given in Table 1.

VLE data on the basis of the cyclohexanone model are presented together with experimental data and the DIPPR correlation [18] in Figures 2 to 4. Note that the DIPPR correlation for the saturated liquid density is based on experimental data that are only available at temperatures below 370 K. The vapor pressure correlation by DIPPR [18] is based on experimental data below 460 K. The agreement between the molecular model and the correlation is good. The mean unsigned errors in vapor pressure, saturated liquid density and enthalpy of vaporization are 2.7, 0.9 and 5.3 %, respectively, in the temperature range from 390 to 620 K, which is about 60 to 95 % of the critical temperature. The relative deviation plot and the numerical simulation results are given in the supplementary material. Table 2 compares the critical properties estimated from simulations to experimental data. The agreement of the critical properties is good, the highest relative deviation was found for the critical density (3 %).

The second virial coefficient from the present model is compared to a prediction by DIPPR [18] in Figure 7. The two data sets differ by around 50 % at low temperatures and by around 30 % at high temperatures. The present numerical results are given in the supplementary material.

3. Molecular Mixture Models

To describe mixtures on the basis of pairwise additive potentials, molecular modeling reduces to the specification of the interaction between un-

like molecules. The unlike polar interactions were treated in a physically straightforward manner without using binary parameters. For the unlike LJ interactions, the modified Lorentz-Berthelot combination rule with one state-independent binary parameter was used [19]

$$\sigma_{AB} = (\sigma_A + \sigma_B)/2, \tag{1}$$

and

$$\epsilon_{AB} = \xi\sqrt{\epsilon_A \epsilon_B}. \tag{2}$$

The binary parameter ξ was adjusted to a single experimental data point (vapor pressure of the mixture or Henry's law constant). Table 3 contains the temperature, mole fraction and experimental vapor pressure or the experimental Henry's law constant which were used for the adjustment as well as the resulting binary parameter ξ and the respective simulation results.

4. Vapor-Liquid Equilibria of the Three Binary Systems

4.1. Carbon Dioxide + Cyclohexane

The VLE of the binary system carbon dioxide + cyclohexane is shown in Figure 8. Present simulation results are compared to experimental data [8, 20, 21, 22] and to the Peng-Robinson (PR) EOS [23] for the three temperatures 313.15, 344.4 and 410.9 K. Carbon dioxide is supercritical at these temperatures. All isotherms exhibit a concave bubble line. At 313.15 K, the agreement between the simulation results and the two experimental data sets [8, 21] is very good. Also the vapor phase composition, which is a fully predictive quantity in the present context, is in good agreement with the PR EOS [23]. For higher temperatures, the simulation results overpredict the vapor pressure of the binary mixture with a maximum deviation at the highest temperature of about 25%. The predicted vapor phase composition exhibits a slightly too large carbojn dioxide content near the critical region of the mixture at higher temperatures.

4.2. Carbon Dioxide + Cyclohexanone

The VLE of the binary system carbon dioxide + cyclohexanone is shown in Figure 9 for a temperature range where carbon dioxide is supercritical. At 313.15 K, an almost straight bubble line and a concave dew line is observed. At 433.5 K, a typical supercritical concave bubble line is seen. For both temperatures, the agreement between the simulation results, the PR EOS [23]

and the experimental data [8, 21, 24, 25] is very good. Only at 433.5 K near the critical region of the mixture, the vapor pressure and the saturated vapor mole fraction of carbon dioxide were slightly overpredicted by simulation.

4.3. Cyclohexane + Cyclohexanone

The VLE for the binary system cyclohexane + cyclohexanone is presented in Figure 10 for the two temperatures 323.15 and 348.15 K. Both isotherms show a S-shaped bubble line. Throughout, the agreement between the simulation results, the PR EOS [23] and the experimental data by Boublik and Lu [26] is excellent.

All numerical simulation results are given in the supplementary material.

5. Henry's Law Constant of Carbon Dioxide in Cyclohexane and in Cyclohexanone

Figure 11 shows the present simulation results for the temperature dependence of the Henry's law constant of carbon dioxide in pure cyclohexane and in pure cyclohexanone, respectively, in comparison with experimental data [8, 27, 28, 29, 30, 31, 32]. For both systems, the Henry's law constant was overpredicted at higher temperatures with a maximum deviation at the highest temperature of 10% and 7.5% for carbon dioxide in cyclohexane and in cyclohexanone, respectively. For lower temperatures, the data from simulation and experiment agree well for both systems.

Predictions of the Henry's law constant of carbon dioxide in the mixture cyclohexane + cyclohexanone are compared to experimental data by Merker et al. [8] in Figure 12 and in Table 4 for three temperatures. For the lowest temperature (315.5 K), the predictions are in an very good agreement with the experimental data over the whole composition range. For the two higher temperatures (352.7 and 392 K), the predictions from simulation are too high. Nevertheless, the qualitative behavior is the same as found by experiment. Note that the deviations between simulation and experiment are due to the deviations in the binary subsystem of carbon dioxide + cyclohexane and carbon dioxide + cyclohexanone. The Henry's law constant of carbon dioxide varies strongly upon addition of small amounts of cyclohexanone to pure cyclohexane, whereas at higher cyclohexanone mole fractions an almost constant Henry's law constant can be observed for a given temperature.

6. Conclusion

In this work, a modified cyclohexane model, based on the work by Eckl et al. [10], was presented. The major difference is the absence of the point quadrupole, the remaining parameters of the new cyclohexane model were adjusted to experimental pure substance VLE data. It was found to be as good as the model by Eckl et al. [10] regarding VLE properties. Predictions of the second virial coefficient as well as of the thermal and caloric properties are in good agreement with a reference EOS [14].

Furthermore, a new cyclohexanone model was proposed. The geometry of the cyclohexanone model is based on QM calculations, whereas the remaining parameters were adjusted to experimental pure substance VLE data. The mean unsigned errors for vapor pressure, saturated liquid density and enthalpy of vaporization are 2.7, 0.9, and 5.3 %, respectively, in the temperature range from 390 to 620 K. The second virial coefficient based on this model differs significantly from a DIPPR prediction.

These two pure substance molecular models were used for the simulation of binary VLE data of carbon dioxide + cyclohexane, carbon dioxide + cyclohexanone and cyclohexane + cyclohexanone using a carbon dioxide model from prior work. The modified Lorentz-Berthelot rule with one state-independent binary parameter ξ was assumed for the unlike LJ interactions. The VLE simulations of the binary mixtures carbon dioxide + cyclohexanone and cyclohexane + cyclohexanone are in a very good agreement with experimental data in the entire composition range, covering a large temperature range. For the binary mixture carbon dioxide + cyclohexane the vapor pressure was overpredicted at higher temperatures.

The predictions of the Henry's law constant of carbon dioxide in the liquid mixture cyclohexane + cyclohexanone shows a very good agreement with experimental data at 315.5 K. At higher temperatures, the Henry's law constant of carbon dioxide was overpredicted, but a qualitatively correct the composition dependence was found.

Acknowledgement

The authors gratefully acknowledge financial support by Deutsche Forschungsgemeinschaft, Collaborative Research Centre SFB 706 "Selective Catalytic Oxidations Using Molecular Oxygen". The presented research was conducted under the auspices of the Boltzmann-Zuse Society of Computational

Molecular Engineering (BZS). The simulations were performed on the national super computer NEC SX-8 at the High Performance Computing Centre Stuttgart (HLRS) under the grant MMHBF and on the HP XC4000 supercomputer at the Steinbruch Centre for Computing under the grant LAMO.

7. Appendix: Simulation Details

In this work, the Grand Equilibrium method [33] was used for VLE simulations. To determine the chemical potential in the liquid, gradual insertion [34] and Widom's insertion method [35] were used. For low temperatures near the triple point, gradual insertion yields results with much lower statistical uncertainties than Widom's method.

Widom's method was applied in conjunction with molecular dynamics simulations in the NpT ensemble using isokinetic velocity scaling [36] and Anderson's barostat [37]. There, the number of molecules was 1372 and the time step was 1 fs. The initial configuration was a face centred cubic lattice, the fluid was equilibrated over 60 000 time steps with the first 10 000 time steps in the canonical (NVT) ensemble. The production run went over 400 000 time steps with a membrane mass of 10^9 kg/m^4. Up to 5 000 test molecules were inserted every production time step.

Gradual insertion was applied in conjunction with Monte Carlo simulations in the NpT ensemble using 1372 molecules. Starting from a face centred cubic lattice, 15 000 Monte Carlo cycles were performed for equilibration with the first 5 000 cycles in the canonical (NVT) ensemble and 100 000 cycles for production. Every 50 cycles, 13 720 fluctuating state change moves, 13 720 fluctuating particle translation/rotation moves and 68 600 biased particle translation/rotation moves were performed to determine the chemical potential.

For the corresponding vapor, Monte Carlo simulations in the pseudo-μVT ensemble were conducted. The simulation volume was adjusted to lead to an average number of 864 molecules in the vapor phase. After 10 000 initial NVT Monte Carlo cycles, starting from a face centred cubic lattice, 25 000 equilibration cycles in the pseudo-μVT ensemble were performed. The length of the production run was 100 000 cycles. One cycle is defined here to be a number of attempts to displace and rotate molecules equal to the actual number of molecules plus three insertion and three deletion attempts.

The cut-off radius was set to at least 15 Å and a center of mass cut-off scheme was employed. Lennard-Jones long-range interactions beyond the

cut-off radius were corrected as proposed by Lustig [36]. Statistical uncertainties of the simulated values were estimated by a block averaging method [38].

For the simulations in the homogeneous region and of the Henry's law constant, molecular dynamics simulations were made with the same technical parameters as used for the liquid runs during VLE calculations using Widom's insertion method [35] to determine the chemical potential for the determinationof the Henry's law constant.

All calculations were performed with the molecular simulation tool $ms2$ [39].

References

[1] F. Case, A. Chaka, D. G. Friend, D. Frurip, J. Golab, R. Johnson, J. Moore, R. D. Mountain, J. Olson, M. Schiller, J. Storer, Fluid Phase Equilib. 217 (2004) 1–10.

[2] F. Case, A. Chaka, D. G. Friend, D. Frurip, J. Golab, P. Gordon, R. Johnson, P. Kolar, J. Moore, R. D. Mountain, J. Olson, R. Ross, M. Schiller, Fluid Phase Equilib. 236 (2005) 1–14.

[3] F. H. Case, J. Brennan, A. Chaka, K. D. Dobbs, D. G. Friend, D. Frurip, P. A. Gordon, J. Moore, R. D. Mountain, J. Olson, R. B. Ross, M. Schiller, V. K. Shen, Fluid Phase Equilib. 260 (2007) 153–163.

[4] F. H. Case, J. Brennan, A. Chaka, K. D. Dobbs, D. G. Friend, P. A. Gordon, J. D. Moore, R. D. Mountain, J. D. Olson, R. B. Ross, M. Schiller, V. K. Shen, E. A. Stahlberg, Fluid Phase Equilib. 274 (2008) 2–9.

[5] F. H. Case, A. Chaka, J. D. Moore, R. D. Mountain, J. D. Olson, R. B. Ross, M. Schiller, V. K. Shen, E. A. Stahlberg, Fluid Phase Equilib. 285 (2009) 1–3.

[6] U. Schuchhardt, W. A. Carvalho, E. V. Spinacé, Synlett 10 (1993) 713–718.

[7] F. Schurz, J. M. Bauchert, T. Merker, T. Schleid, H. Hasse, R. Gläser, App. Catal. A 355 (2009) 42–49.

[8] T. Merker, N. Franke, R. Gläser, T. Schleid, H. Hasse, J. Chem. Eng. Data 56 (2011) 2477–2481.

[9] T. Merker, C. Engin, J. Vrabec, H. Hasse, J. Chem. Phys. 132 (2010) 234512.

[10] B. Eckl, J. Vrabec, H. Hasse, J. Phys. Chem. B 112 (2008) 12710–12721.

[11] Y.-L. Huang, M. Heilig, H. Hasse, J. Vrabec, AIChE J. 52 (2010) 1043–1060.

[12] J. Stoll, Molecular Models for the Prediction of Thermophysical Properties of Pure Fluids and Mixtures, Reihe 3, VDI-Verlag, Düsseldorf, 2005.

[13] T. Merker, J. Vrabec, H. Hasse, Soft Materials (2011) accepted.

[14] S. G. Penoncello, A. R. H. Goodwin, R. T. Jacobsen, Int. J. Thermophys. 16 (1995) 519–531.

[15] A. Lotfi, J. Vrabec, J. Fischer, Mol. Phys. 76 (1992) 1319–1333.

[16] E. Taskinen, J. Phys. Org. Chem. 23 (2010) 105–114.

[17] M. W. Schmidt, K. K. Baldridge, J. A. Boatz, S. T. Elbert, M. S. Gordon, J. H. Jensen, S. Koseki, N. Matsunaga, K. A. Nguyen, S. Su, T. L. Windus, M. Dupuis, J. A. Montgomery, J. Comput. Chem. 14 (1993) 1347–1363.

[18] R. L. Rowley, W. V. Wilding, J. L. Oscarson, Y. Yang, N. A. Zundel, T. E. Daubert, R. P. Danner, DIPPR® Data Compilation of Pure Compound Properties, Design Institute for Physical Properties, AIChE, New York, 2006.

[19] T. Schnabel, J. Vrabec, H. Hasse, J. Mol. Liq. 135 (2007) 170–178.

[20] N. Nagarajan, R. L. J. Robinson, J. Chem. Eng. Data 32 (1987) 369–371.

[21] M. C. Esmelindro, O. A. C. Antunes, E. Franceschi, G. R. Borges, M. L. Corazza, J. V. Oliveira, W. Linhares, C. Dariva, J. Chem. Eng. Data 53 (2008) 2050–2055.

[22] S. K. Shibata, S. I. Sandler, J. Chem. Eng. Data 34 (1989) 419–424.

[23] D. Y. Peng, D. B. Robinson, Ind. Chem. Eng. Fundam. 15 (1976) 59–64.

[24] Y. Feng, W. Hu, Y. Hou, Gaoxiao Huaxue Gongcheng Xuebao 6 (1992) 19–24.

[25] S. Laugier, D. Richon, J. Chem. Eng. Data 42 (1997) 155–159.

[26] T. Boublik, B. C. Y. Lu, J. Chem. Eng. Data 22 (1977) 331–333.

[27] F. Gironi, R. Lavecchia, Fluid Phase Equilib. 87 (1993) 153–161.

[28] L. Patyi, I. E. Furmer, J. Makranczy, A. S. Sadilenko, Z. G. Stepanova, M. G. Berengarten, J. Applied Chem. (Russ.) 51 (1978) 1240–1243.

[29] E. Wilhelm, R. Battino, J. Chem. Thermodyn. 5 (1973) 117–120.

[30] J. Dymond, J. Phys. Chem. 71 (1967) 1829–1831.

[31] M. Gallardo, J. Melendo, J. Urieta, C. Guitierrez Losa, Can. J. Chem. 65 (1987) 2198–2202.

[32] J. Melendo, M. Gallardo, J. Urieta, C. Gutierrez Losa, Acta Cient. Compostelana 12 (1985) 269–284.

[33] J. Vrabec, H. Hasse, Mol. Phys. 100 (2002) 3375–3383.

[34] J. Vrabec, M. Kettler, H. Hasse, Chem. Phys. Lett. 356 (2002) 431–436.

[35] B. Widom, J. Chem. Phys. 39 (1963) 2808–2812.

[36] M. P. Allen, D. J. Tildesley, Computer simulations of liquids, Clarendon Press, Oxford, 1987.

[37] H. C. Anderson, J. Chem. Phys. 72 (1980) 2384–2393.

[38] H. Flyvbjerg, H. G. Petersen, J. Chem. Phys. 91 (1989) 461–466.

[39] S. Deublein, B. Eckl, J. Stoll, S. V. Lishchuk, G. Guevara-Carrion, C. W. Glass, T. Merker, M. Bernreuther, H. Hasse, J. Vrabec, Comp. Phys. Commun. (2011) doi:10.1016/j.cpc.2011.04.026.

Table 1: Coordinates and parameters of the LJ sites in the principal axes system of the cyclohexane and cyclohexanone models. The orientation of the dipole is defined in standard Euler angles, where φ is the azimuthal angle with respect to the $x-z$ plane and θ is the inclination angle with respect to the z axis.

Interaction Site	x Å	y Å	z Å	σ Å	ε/k_B K	φ deg	θ deg	μ D
Cyclohexane								
CH$_2$(1)	0.2994	-1.5343	-0.8878	3.490	87.6	—	—	—
CH$_2$(2)	-0.2994	-1.5343	0.8878	3.490	87.6	—	—	—
CH$_2$(3)	-0.3123	-0.0210	-1.8082	3.490	87.6	—	—	—
CH$_2$(4)	-0.2988	1.5553	1.0002	3.490	87.6	—	—	—
CH$_2$(5)	0.2988	1.5553	-1.0002	3.490	87.6	—	—	—
CH$_2$(6)	-0.3123	-0.0210	-1.8082	3.490	87.6	—	—	—
Cyclohexanone								
CH$_2$(1)	0.5579	-1.5761	-0.5402	3.424	140.6	—	—	—
CH$_2$(2)	-0.5078	-1.5582	1.1954	3.424	140.6	—	—	—
CH$_2$(3)	0.3603	0	2.1671	3.424	140.6	—	—	—
CH$_2$(4)	-0.5078	1.5582	1.1954	3.424	140.6	—	—	—
CH$_2$(5)	0.5579	1.5761	-0.5402	3.424	140.6	—	—	—
C	0.0203	0	-1.1120	2.789	10.3	—	—	—
O	-0.4181	0	-2.2087	3.108	34.1	—	—	—
dipole	-0.1989	0	-1.6604	—	—	0	21.79	2.554

Table 2: Critical properties of the pure substances on the basis of the molecular models in comparison to experimental data.

	T_c^{sim} K	T_c^{exp} K	ρ_c^{sim} mol/l	ρ_c^{exp} mol/l	p_c^{sim} MPa	p_c^{exp} MPa	Ref.
Cyclohexane	557	553.8	3.258	3.244	4.299	4.08	[14]
Cyclohexanone	650.85	653	3.122	3.216	4.046	3.988	[18]

Table 3: Binary interaction parameter ξ, experimental bubble point or Henry's law constant used for the adjustment with reference, simulation results with adjusted ξ and binary parameter k_{ij} of the Peng-Robinson EOS. The number in parentheses indicates the statistical uncertainty in the last digit.

Mixture (1 + 2)	ξ	T	x_1	p^{exp}/H_1^{exp}	p^{sim}/H_1^{sim}	y_1^{sim}	k_{ij}
		K	mol/mol	MPa	MPa	mol/mol	
Carbon dioxide + Cyclohexane	0.95	313.15		16.2 [8]	15.8 (4)		0.1415
Carbon dioxide + Cyclohexanone	1.02	313.15		8.5 [8]	8.7 (9)		0.0325
Cyclohexane + Cyclohexanone	0.982	348.15	0.442	0.058 [26]	0.058(2)	0.933(4)	0.0555

Table 4: Prediction of the Henry's law constant of carbon dioxide (1) in cyclohexane (2) + cyclohexanone (3). x_3' is the mole fraction of cyclohexanone (3) (on a carbon dioxide-free basis). The number in parentheses indicates the uncertainty in the last digit.

	T=315.5 K	T=352.7 K	T=392 K
$x_3^{'}$ / mol mol^{-1}	$H_{1,2+3}$ / MPa	$H_{1,2+3}$ / MPa	$H_{1,2+3}$ / MPa
0	15.8(4)	21.2(3)	25.0(3)
0.1	14.0(4)	19.1(3)	23.6(2)
0.2	12.4(4)	17.8(3)	22.4(2)
0.3	11.6(4)	17.0(3)	21.7(2)
0.4	10.6(5)	16.6(3)	20.9(2)
0.5	10.1(5)	15.7(3)	20.5(2)
0.6	9.7(7)	15.2(3)	20.3(3)
0.7	9.5(7)	14.8(4)	20.0(3)
0.8	9.1(7)	14.6(4)	20.1(3)
0.9	8.6(8)	14.4(5)	20.2(3)
1	8.7(9)	14.4(5)	20.1(3)

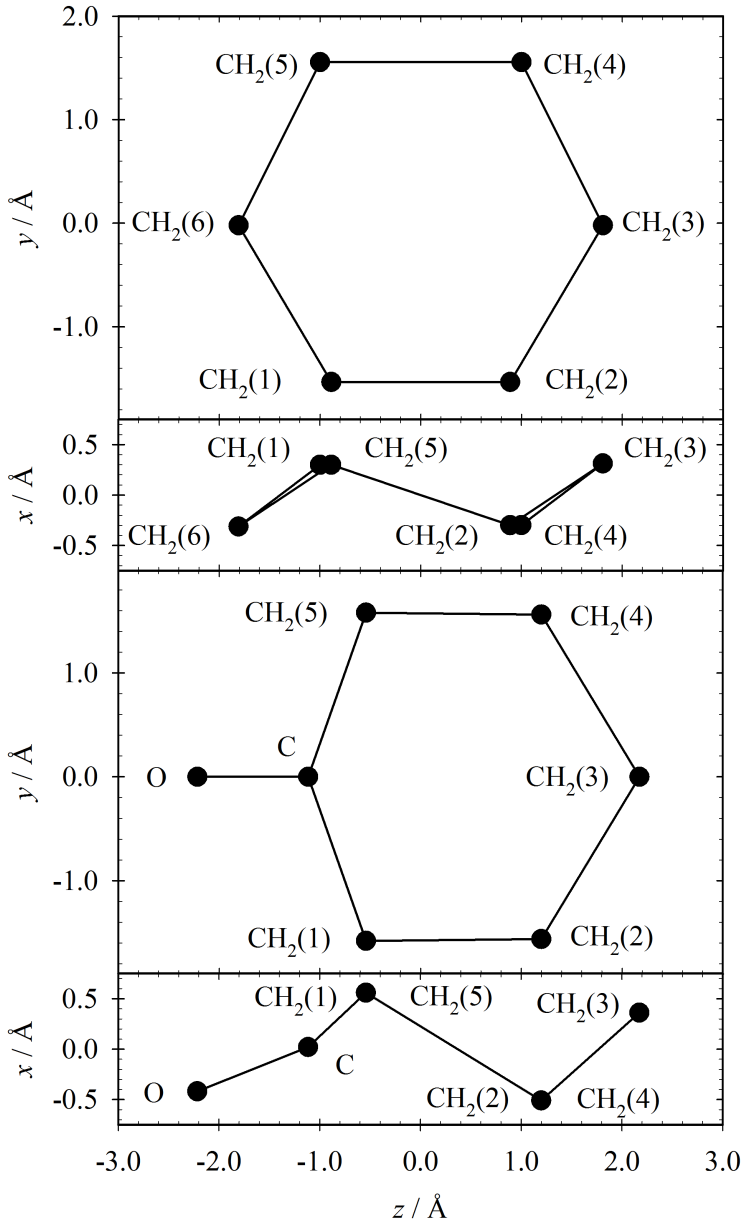

Figure 1: Coordinates of the LJ sites of the present molecular models. Top: cyclohexane, bottom: cyclohexanone.

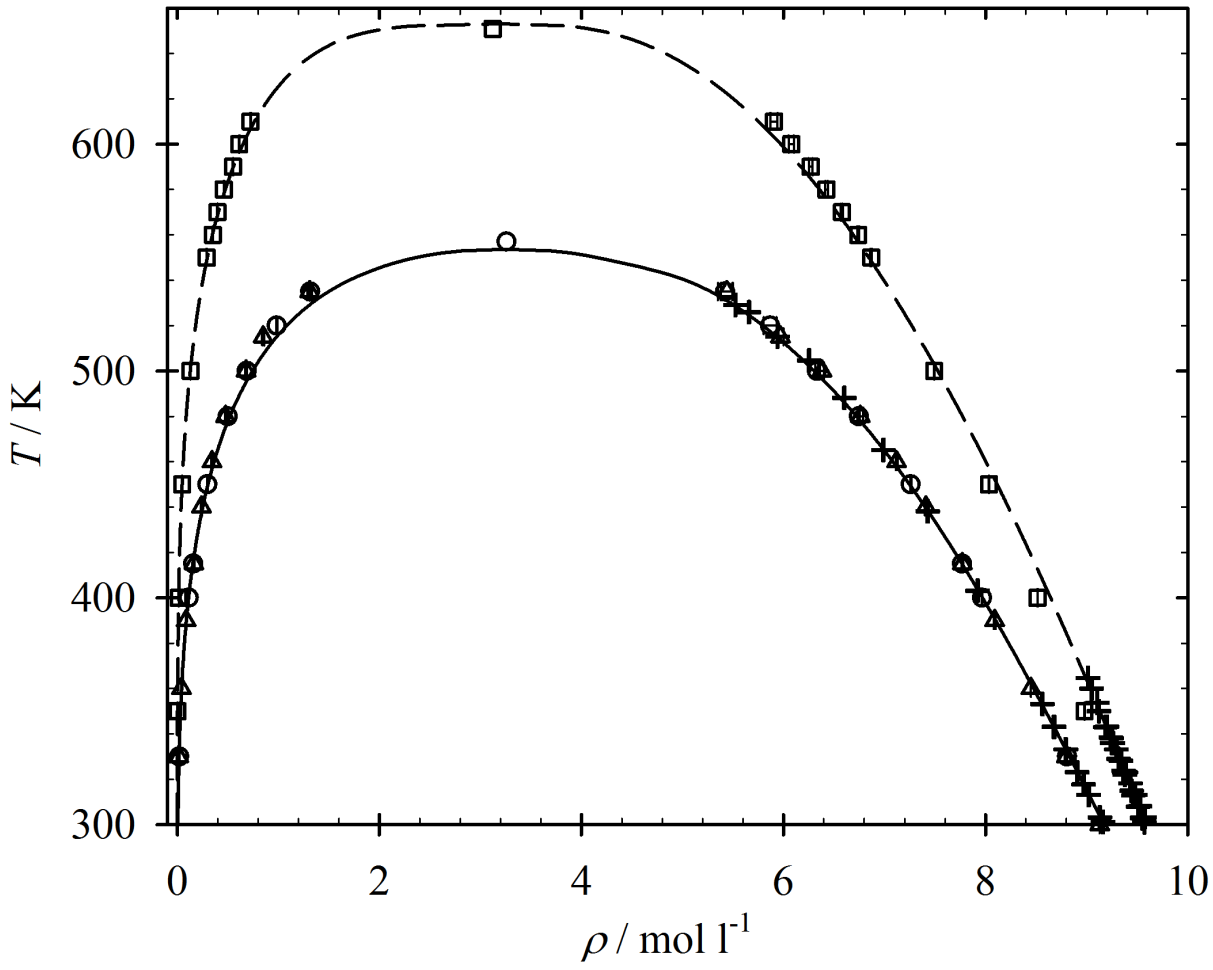

Figure 2: Saturated densities. Present simulation data: ○ cyclohexane, this work; □ cyclohexanone, this work; △ cyclohexane model by Eckl et al. [10]; — reference EOS [14]; - - DIPPR correlation [18]; + experimental data from the DIPPR database [18]. The empty symbols without error bars indicate the critical point.

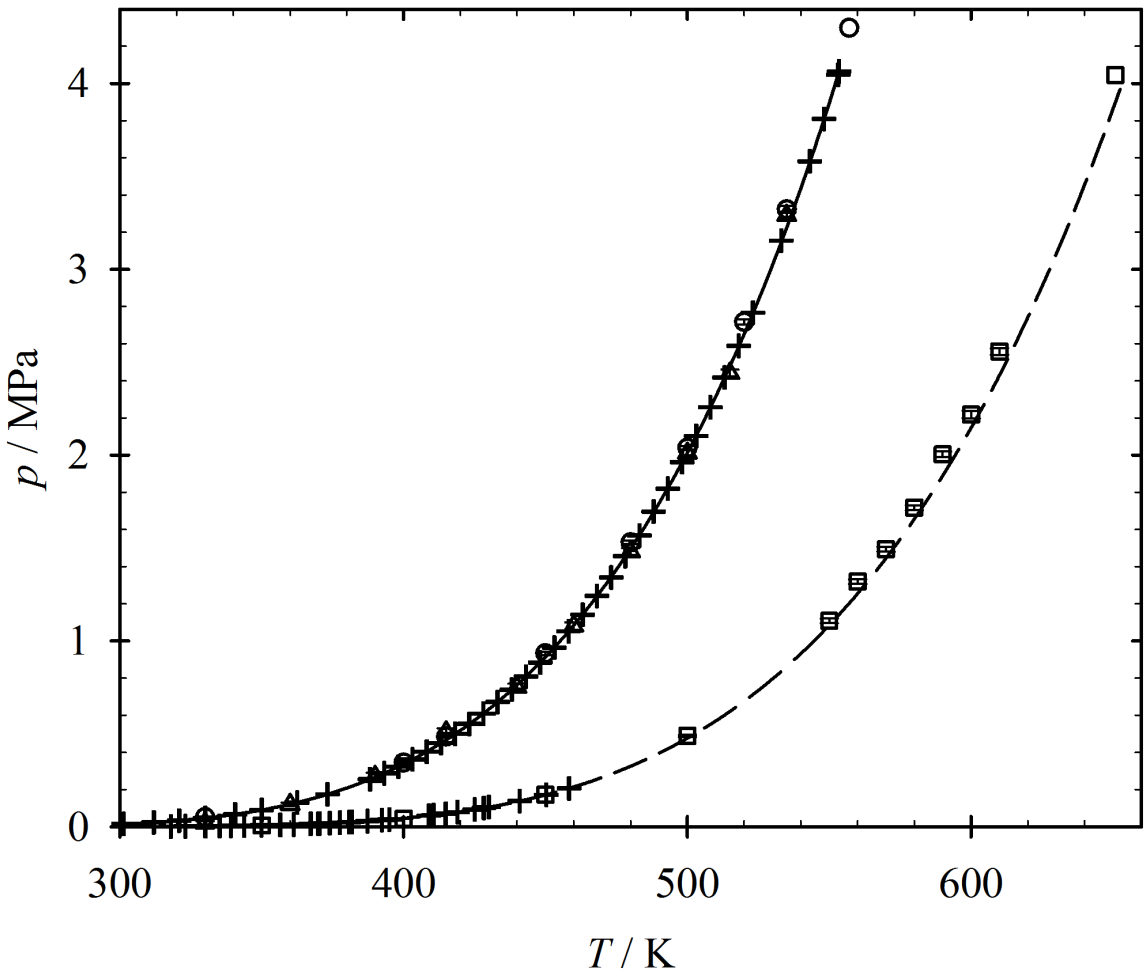

Figure 3: Vapor pressure. Present simulation data: ○ cyclohexane, this work; □ cyclohexanone, this work; △ cyclohexane model by Eckl et al. [10]; — reference EOS [14]; - - DIPPR correlation [18]; + experimental data from the DIPPR database [18]. The empty symbols without error bars at the top indicate the critical point.

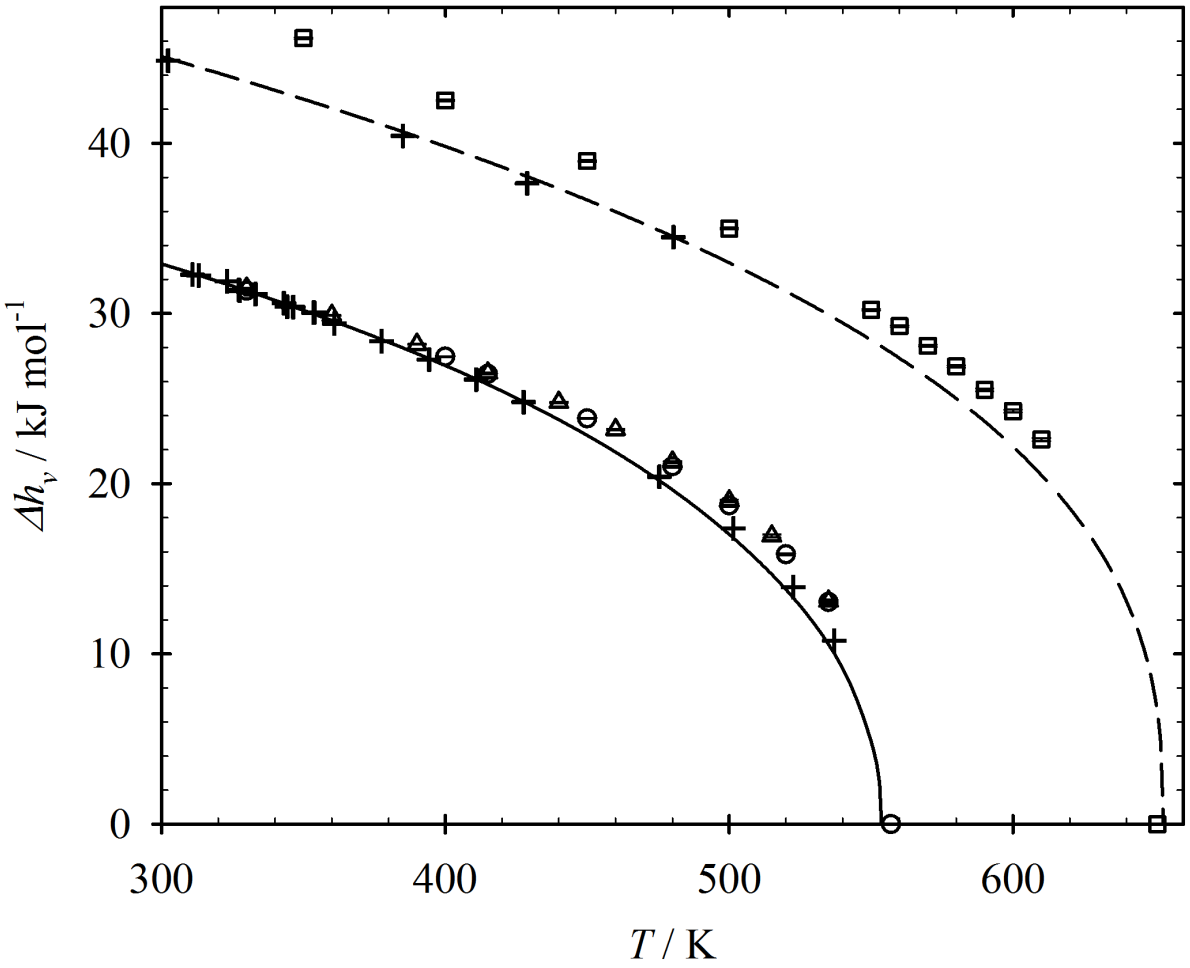

Figure 4: Enthalpy of vaporization. Present simulation data: ○ cyclohexane, this work; □ cyclohexanone, this work; △ cyclohexane model by Eckl et al. [10]; — reference EOS [14]; - - DIPPR correlation [18]; + experimental data from the DIPPR database [18]. The empty symbols without error bars at the bottom indicate the critical point.

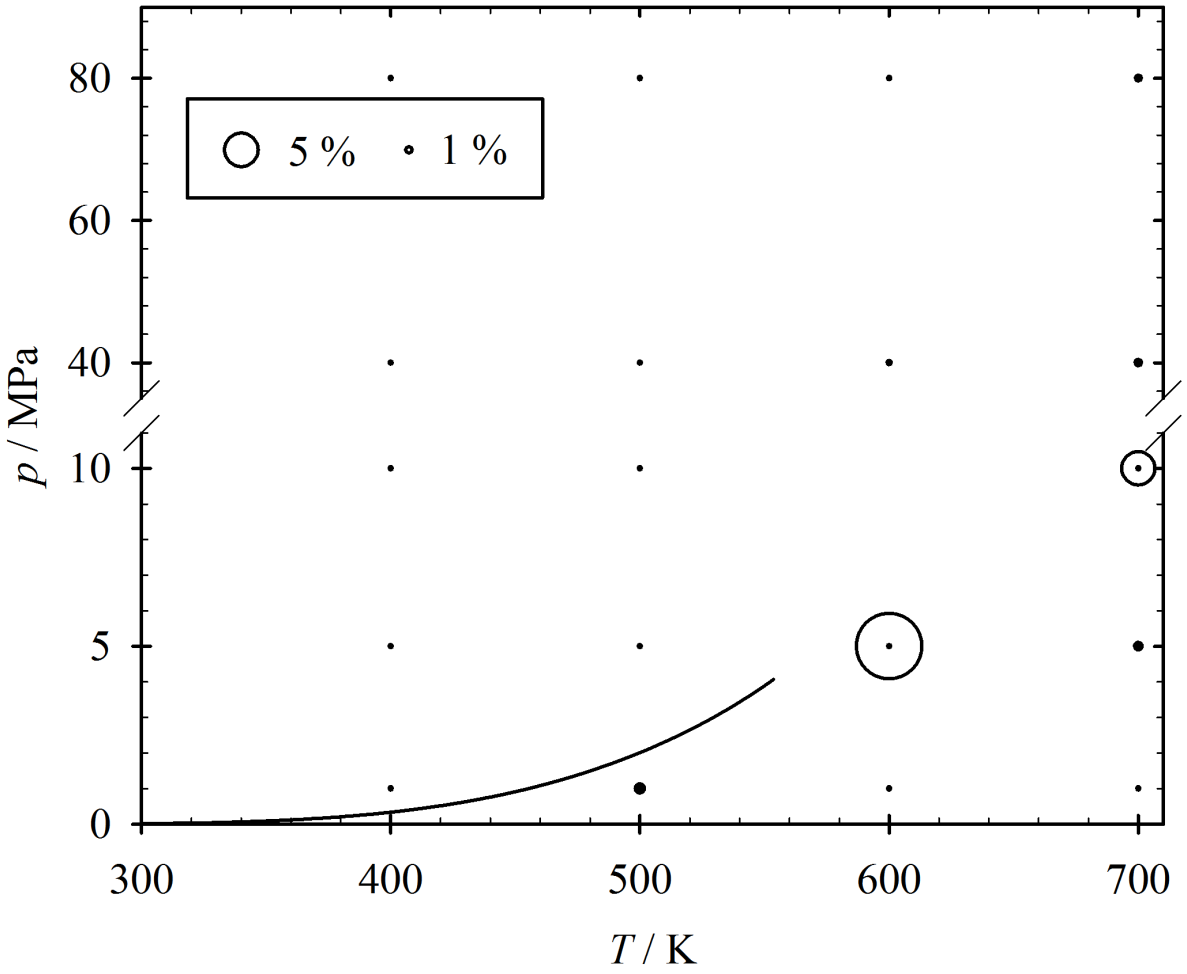

Figure 5: Relative deviations between simulation data and reference EOS [14] for the density ($\delta\rho = (\rho_{\mathrm{sim}} - \rho_{\mathrm{EOS}})/\rho_{\mathrm{EOS}}$) in the homogeneous fluid region of cyclohexane: ○ present simulation data; — vapor pressure curve [14]. The size of the bubbles indicates the magnitude of the relative deviations.

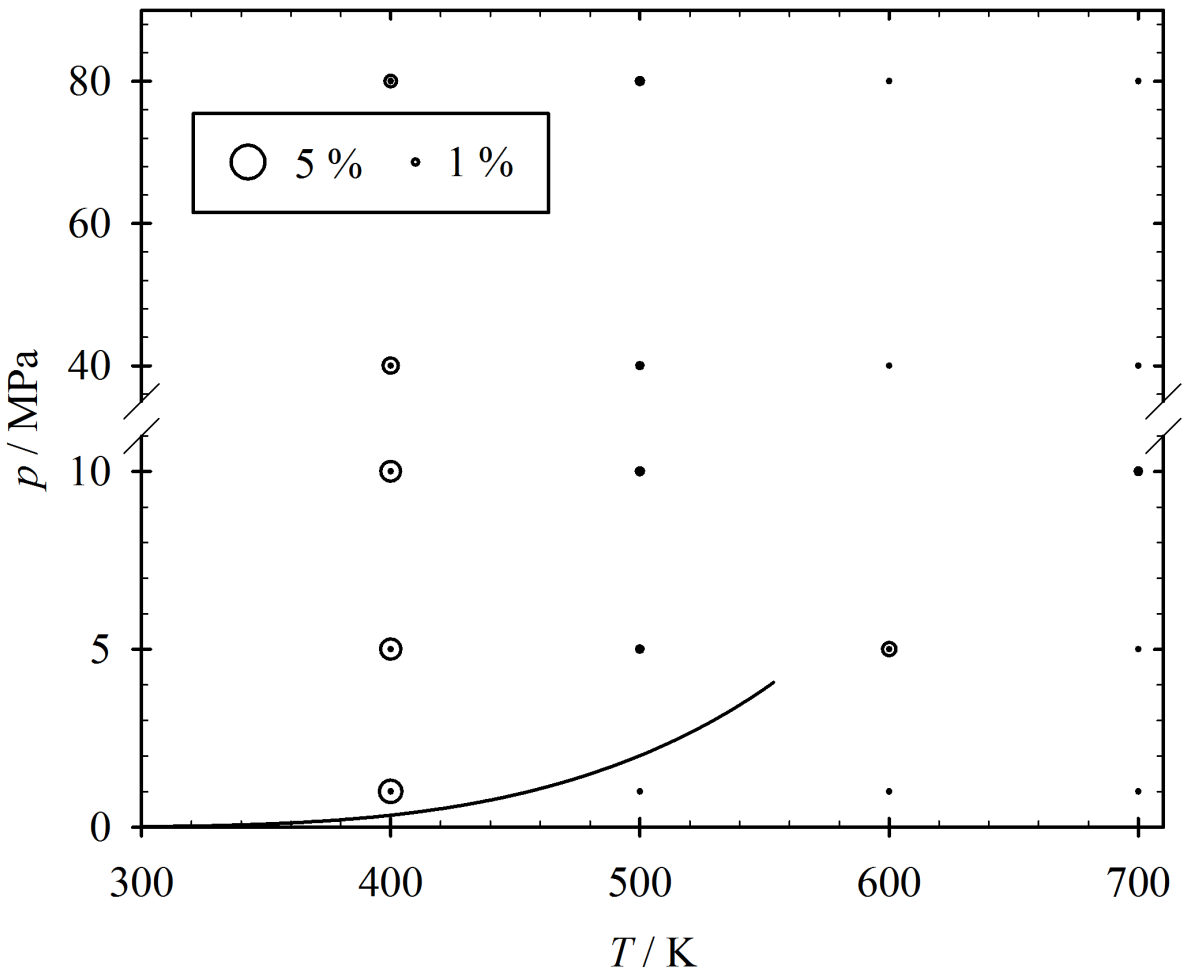

Figure 6: Relative deviations between simulation data and reference EOS [14] for the residual enthalpy ($\delta h^{\mathrm{res}} = (h^{\mathrm{res}}_{\mathrm{sim}} - h^{\mathrm{res}}_{\mathrm{EOS}})/h^{\mathrm{res}}_{\mathrm{EOS}}$) in the homogeneous fluid region of cyclohexane: ○ present simulation data; — vapor pressure curve [14]. The size of the bubbles indicates the magnitude of the relative deviations.

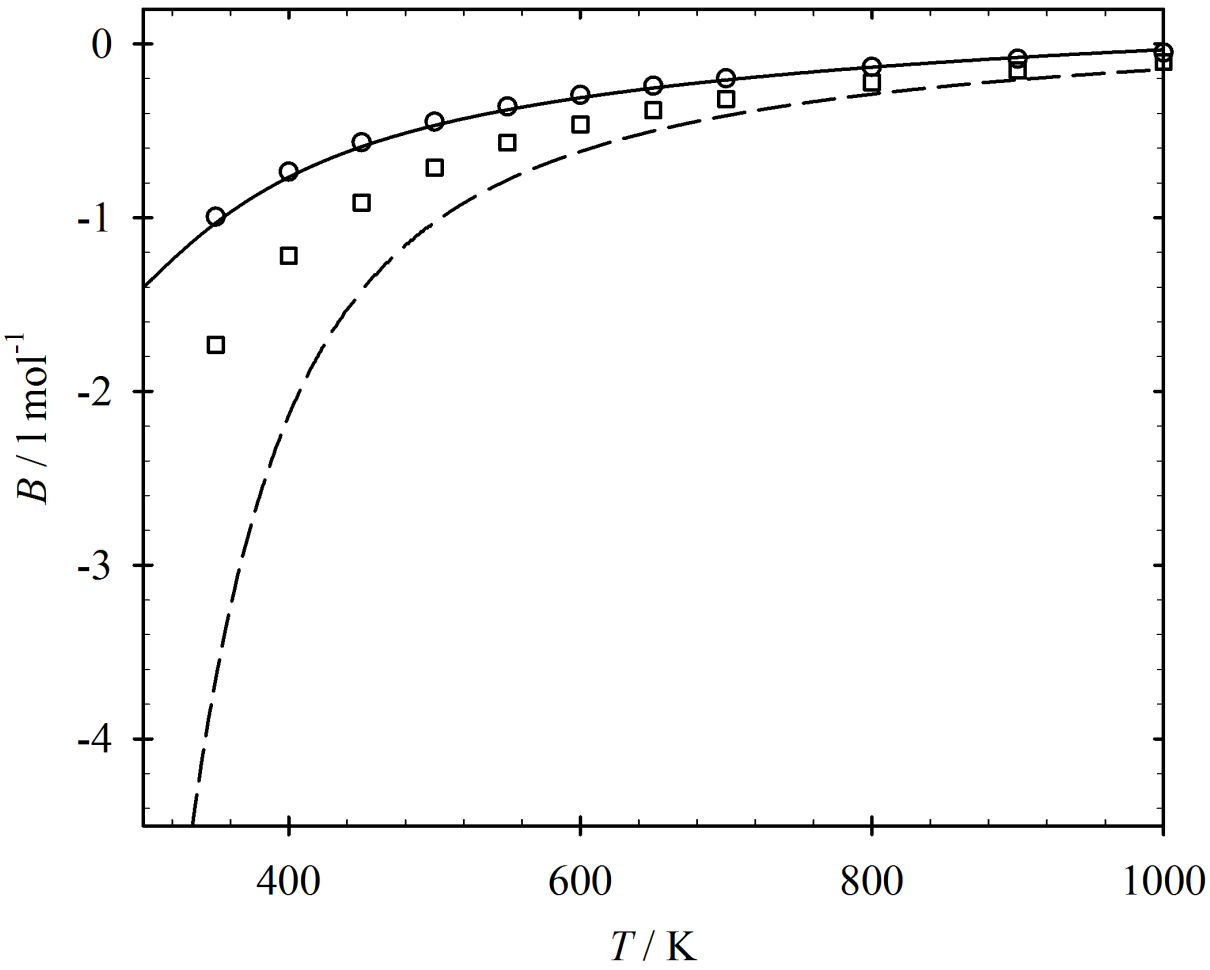

Figure 7: Second virial coefficient. Present data: ○ cyclohexane; □ cyclohexanone; — reference EOS [14]; - - DIPPR correlation [18].

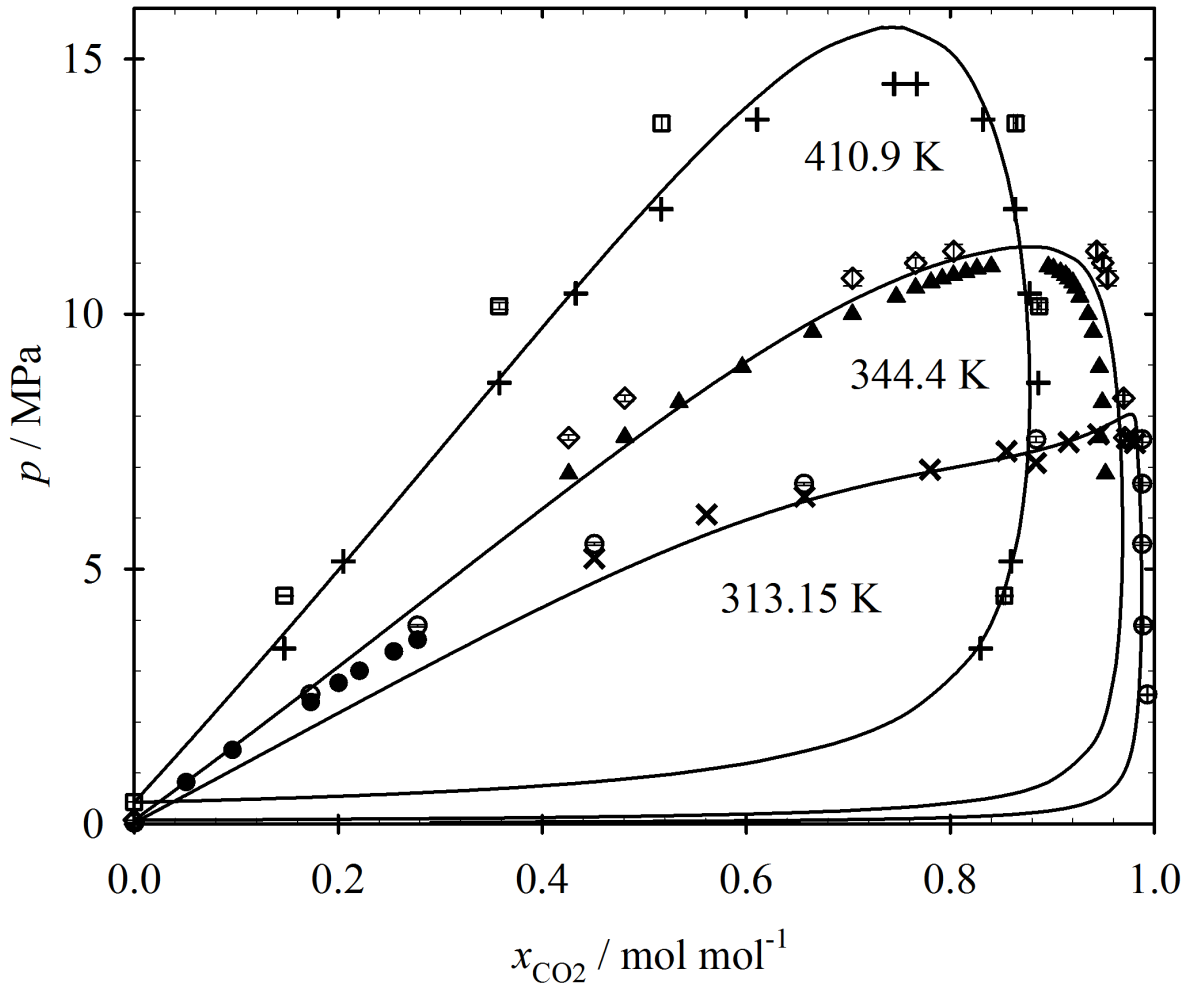

Figure 8: Isothermal vapor-liquid phase diagram of carbon dioxide + cyclohexane at 313.15, 344.4 and 410.9 K: + experimental data by Shibata and Sandler [22]; × experimental data by Esmelindro et al. [21]; ▲ experimental data by Nagarajan and Robinson [20]; ● experimental data by Merker et al. [8]; ○, ◇, □ present simulation data with $\xi = 0.95$; —— Peng-Robinson EOS [23] with $k_{ij} = 0.12$.

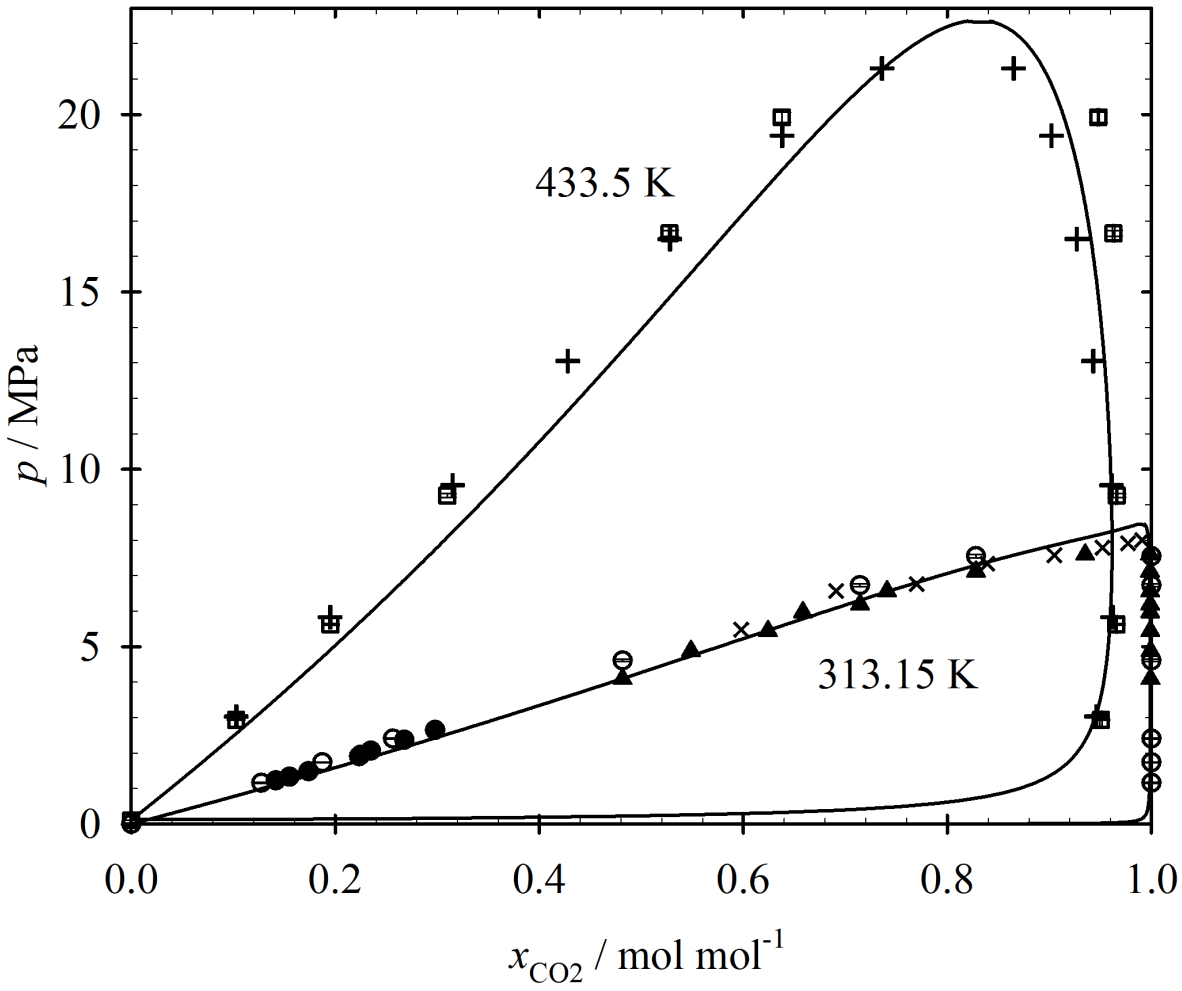

Figure 9: Isothermal vapor-liquid phase diagram of carbon dioxide + cyclohexanone at 313.15 and 433.5 K: + experimental data by Laugier and Richon [25]; × experimental data by Esmelindro et al. [21]; ▲ experimental data by Feng et al. [24]; ● experimental data by Merker et al. [8]; ○, □ present simulation data with $\xi = 1.02$; —— Peng-Robinson EOS [23] with $k_{ij} = 0.0325$.

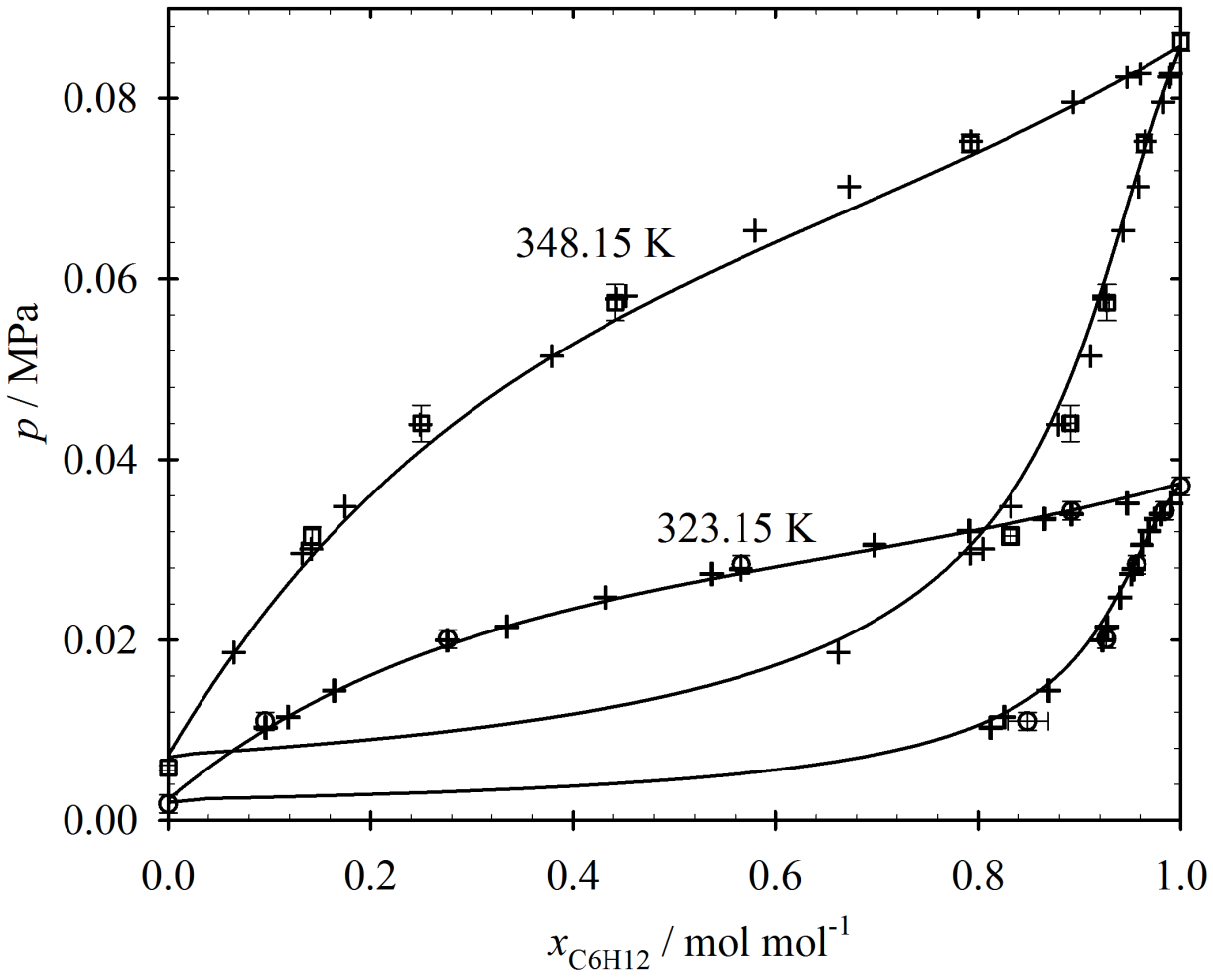

Figure 10: Isothermal vapor-liquid phase diagram of cyclohexane + cyclohexanone at 323.15 and 348.15 K: + experimental data by Boublik and Lu [26]; ○, □ present simulation data with $\xi = 0.982$; —— Peng-Robinson EOS [23] with $k_{ij} = 0.0555$.

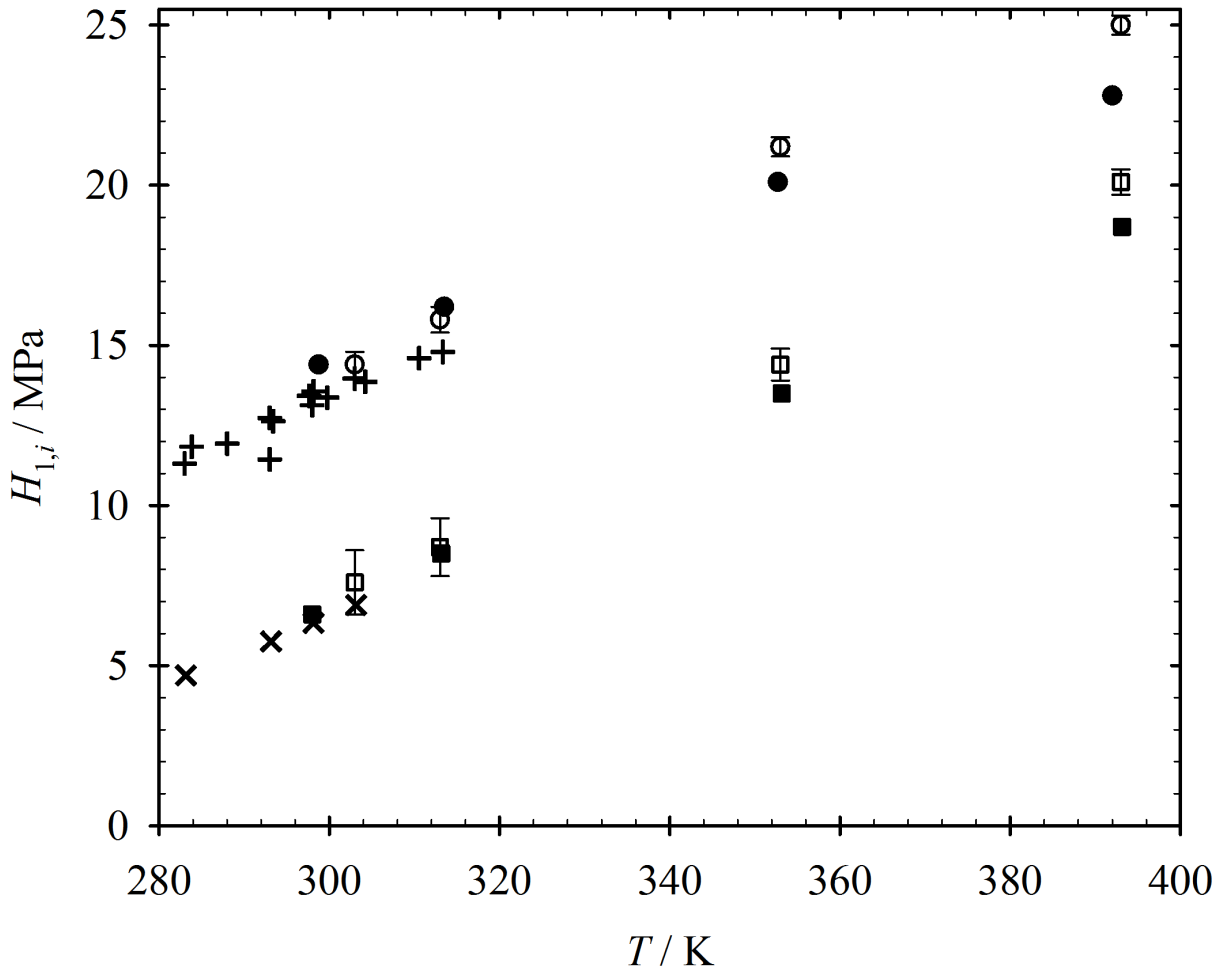

Figure 11: Henry's law constant $H_{1,2}$ of carbon dioxide (1) in cyclohexane (2): ● experimental data by Merker et al. [8]; + other experimental data [27, 28, 29, 30]; ○ present simulation data. Henry's law constant $H_{1,3}$ of carbon dioxide (1) in cyclohexanone (3): ■ experimental data by Merker et al. [8]; × other experimental data [31, 32]; □ present simulation data.

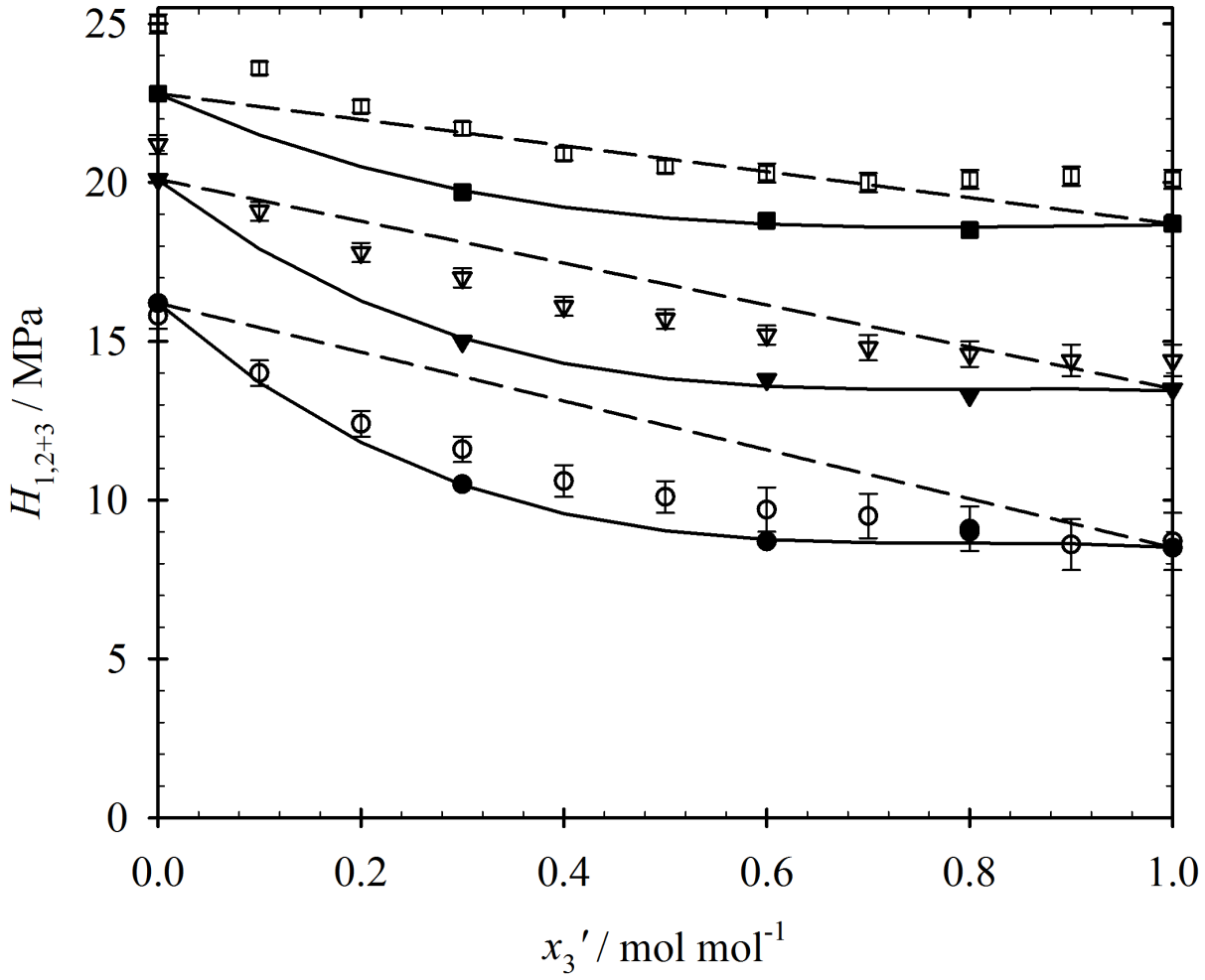

Figure 12: Henry's law constant $H_{1,2+3}$ of carbon dioxide (1) in the mixture cyclohexane (2) + cyclohexanone (3) as a function of the mole fraction x_3' of cyclohexanone (3) (on a carbon dioxide-free basis) at different temperatures: ○ 315.5 K; ▽ 352.7 K; □ 392 K. Open symbols: present simulation data. Full symbols: experimental data by Merker et al. [8]. Solid lines: guides for the eye. Dashed lines: interpolation according to $\ln H_{1,2+3} = x_2' \ln H_{1,2} + x_3' \ln H_{1,3}$.

Supporting Information to: Molecular simulation study on the solubility of Carbon Dioxide in mixtures of Cyclohexane + Cyclohexanone

T. Merker[a], J. Vrabec[b], H. Hasse[a,*]

[a] *Laboratory of Engineering Thermodynamics, University of Kaiserslautern, 67663 Kaiserslautern, Germany*
[b] *Thermodynamics and Energy Technology, University of Paderborn, 33098 Paderborn, Germany*

Abstract

This supplementary material contains the full numerical pure substance simulation data for the vapor-liquid equilibria and the second virial coefficient of the cyclohexane and cyclohexanone models presented in this work. Furthermore, the numerical simulation data for the vapor-liquid equilibria of the three binary mixtures carbon dioxide + cyclohexane, carbon dioxide + cyclohexanone and cyclohexane + cyclohexanone are presented. The relative deviations of vapor-liquid equilibrium properties between simulation data and a reference EOS [1] or a DIPPR correlation [2] are shown for the present cyclohexane and cyclohexanone models and for the cyclohexane model by Eckl et al. [3].

*Corresponding author: Hans Hasse
Technische Universität Kaiserslautern, Lehrstuhl für Thermodynamik, Erwin-Schrödinger-Straße 44, 67663 Kaiserslautern, Germany, *phone* +49 631 205 3464, *fax* +49 631 205 3835
Email address: hans.hasse@mv.uni-kl.de (H. Hasse)
URL: thermo.mv.uni-kl.de (H. Hasse)

Preprint submitted to Fluid Phase Equilibria *July 21, 2011*

Table 1: Vapor-liquid equilibria of cyclohexane: simulation results (sim) are compared to a reference EOS [1] for vapor pressure, saturated densities and enthalpy of vaporization. The number in parentheses indicates the statistical uncertainty in the last digit.

T	p_{sim}	p_{EOS}	ρ'_{sim}	ρ'_{EOS}	ρ''_{sim}	ρ''_{EOS}	$\Delta h_{\mathrm{v,sim}}$	$\Delta h_{\mathrm{v,EOS}}$
K	MPa	MPa	mol/l	mol/l	mol/l	mol/l	kJ/mol	kJ/mol
330	0.051(3)	0.047	8.807(2)	8.831	0.019(1)	0.017	31.334(4)	31.339
400	0.345(5)	0.337	7.966(3)	7.970	0.113(1)	0.112	27.458(7)	26.944
415	0.485(5)	0.467	7.767(4)	7.767	0.157(1)	0.154	26.441(8)	25.828
450	0.933(8)	0.913	7.260(6)	7.247	0.298(1)	0.303	23.84 (1)	22.84
480	1.530(9)	1.496	6.746(9)	6.723	0.500(3)	0.520	21.02 (2)	19.65
500	2.04 (1)	2.01	6.33 (2)	6.30	0.687(4)	0.744	18.72 (2)	17.03
520	2.72 (1)	2.65	5.87 (6)	5.80	0.983(5)	1.083	15.85 (4)	13.79
535	3.32 (2)	3.22	5.42 (7)	5.28	1.315(7)	1.50	13.05 (5)	10.57

Table 2: Vapor-liquid equilibria of cyclohexanone: simulation results (sim) are compared to DIPPR correlations [2] for vapor pressure, saturated densities and enthalpy of vaporization. The number in parentheses indicates the statistical uncertainty in the last digit.

T	p_{sim}	p_{DIPPR}	ρ'_{sim}	ρ'_{DIPPR}	ρ''_{sim}	ρ''_{DIPPR}	$\Delta h_{\mathrm{v,sim}}$	$\Delta h_{\mathrm{v,DIPPR}}$
K	MPa	MPa	mol/l	mol/l	mol/l	mol/l	kJ/mol	kJ/mol
350	0.0074(6)	0.0076	8.980(1)	9.132	0.0026(1)	0.0026	46.17(4)	42.59
400	0.043 (2)	0.0455	8.516(2)	8.644	0.0132(1)	0.0139	42.52(4)	39.81
450	0.173 (3)	0.1711	8.034(2)	8.116	0.0485(1)	0.0482	38.96(5)	36.66
500	0.489 (6)	0.4764	7.492(3)	7.528	0.1299(2)	0.1292	34.99(5)	32.98
550	1.11 (1)	1.0835	6.867(7)	6.846	0.2906(8)	0.2981	30.22(5)	28.44
560	1.32 (1)	1.2539	6.740(8)	6.692	0.350 (1)	0.3488	29.26(5)	27.37
570	1.49 (1)	1.4437	6.58 (1)	6.529	0.397 (1)	0.4075	28.10(6)	26.23
580	1.72 (1)	1.6544	6.43 (1)	6.357	0.460 (1)	0.4758	26.89(7)	25.00
590	2.00 (2)	1.8876	6.27 (2)	6.173	0.550 (2)	0.5559	25.52(8)	23.66
600	2.22 (2)	2.1449	6.08 (3)	5.973	0.612 (3)	0.6508	24.26(8)	22.18
610	2.56 (2)	2.4281	5.91 (3)	5.753	0.726 (5)	0.7653	22.59(9)	20.51

Table 3: Second virial coefficient of cyclohexane and cyclohexanone: present results are compared to a reference EOS [1] and a predictive model by DIPPR [2].

	Cyclohexane		Cyclohexanone	
T	B	B_{EOS}	B	B_{DIPPR}
K	l/mol	l/mol	l/mol	l/mol
350	-0.995	-1.030	-1.732	-3.61
400	-0.735	-0.768	-1.220	-2.14
450	-0.566	-0.592	-0.914	-1.42
500	-0.448	-0.470	-0.721	-1.03
550	-0.361	-0.380	-0.569	-0.78
600	-0.294	-0.310	-0.464	-0.62
650	-0.241	-0.254	-0.382	-0.50
700	-0.198	-0.208	-0.318	-0.41
800	-0.133	-0.135	-0.222	-0.29
900	-0.086	-0.079	-0.154	-0.21
1000	-0.050	-0.034	-0.105	-0.15

Table 4: Vapor-liquid equilibrium simulation results for binary mixtures in partial comparison to experimental vapor pressure data. The number in parentheses indicates the statistical uncertainty in the last digit.

T	x_1	p	p^{exp}	y_1	ρ'	ρ''	Δh_v
K	mol/mol	MPa	MPa	mol/mol	mol/l	mol/l	kJ/mol
Carbon dioxide (1) + Cyclohexane (2)							
313.15	0.0	0.025(5)	0.025 [1]	0	9.001(1)	0.0097(2)	32.179(6)
313.15	0.173	2.54 (1)	2.38 [4]	0.994 (1)	9.918(2)	1.094 (5)	26.913(9)
313.15	0.277	3.89 (2)	3.61 [4]	0.9899(4)	10.564(3)	1.820 (9)	23.721(9)
313.15	0.451	5.49 (3)	5.21 [5]	0.9886(5)	11.790(4)	2.90 (2)	18.79 (2)
313.15	0.657	6.67 (3)	6.42 [5]	0.9888(5)	13.507(8)	4.01 (2)	13.49 (2)
313.15	0.884	7.54 (6)	7.08 [5]	0.9886(4)	15.02 (7)	5.27 (4)	7.66 (5)
344.4	0.0	0.078(1)	0.074 [1]	0	8.652(1)	0.0282(3)	30.632(6)
344.4	0.426	7.58 (5)	6.87 [6]	0.9709(6)	10.96 (1)	3.66 (3)	17.49 (6)
344.4	0.481	8.65 (6)	7.59 [6]	0.9701(7)	11.32 (1)	4.23 (3)	15.79 (2)
344.4	0.704	10.7 (2)	9.99 [6]	0.954 (1)	12.63 (8)	6.9 (1)	8.76 (6)
344.4	0.803	11.2 (1)	10.76 [6]	0.943 (2)	12.6 (2)	8.1 (1)	5.5 (1)
344.4	0.839	11.6 (4)	10.93 [6]	0.942 (2)	12.6 (6)	8.6 (1)	4.4 (2)
410.9	0.0	0.436(5)	0.43 [1]	0	7.823(3)	0.142 (2)	26.75 (1)
410.9	0.147	4.48 (2)	3.44 [7]	0.854 (2)	8.37 (2)	1.481 (6)	22.57 (2)
410.9	0.358	10.16 (7)	8.65 [7]	0.888 (2)	9.19 (8)	3.84 (3)	15.56 (5)
410.9	0.517	13.7 (1)	11.05 [7]	0.864 (3)	9.7 (2)	5.91 (6)	10.05 (9)
Carbon dioxide (1) + Cyclohexanone (2)							
313.15	0.0	0.0013(1)	0.001 [2]	0	9.305(1)	0.0005(1)	46.531(8)
313.15	0.127	1.16 (1)	–	1	10.067(1)	0.467 (4)	41.728(7)
313.15	0.187	1.74 (2)	–	1	10.465(2)	0.721 (6)	39.415(9)
313.15	0.256	2.41 (2)	–	1	10.969(1)	1.027 (8)	36.745(7)
313.15	0.482	4.61 (3)	4.09 [8]	1	12.948(4)	2.24 (2)	27.89 (1)
313.15	0.714	6.73 (4)	6.19 [8]	1	15.606(7)	3.93 (2)	18.40 (2)
313.15	0.828	7.56 (5)	7.12 [8]	0.9997(1)	16.89 (2)	4.99 (3)	13.44 (4)
433.5	0.0	0.111 (1)	0.113 [2]	0	8.191(2)	0.0321(4)	39.212(9)
433.5	0.103	2.95 (2)	3.03 [9]	0.951 (1)	8.663(2)	0.858 (4)	35.47 (1)
433.5	0.195	5.62 (3)	5.83 [9]	0.965 (1)	9.126(3)	1.700 (8)	31.77 (1)
433.5	0.309	9.26 (5)	9.55 [9]	0.966 (1)	9.752(7)	2.95 (2)	27.04 (2)
433.5	0.528	16.65 (8)	16.49 [9]	0.962 (1)	11.02 (2)	5.88 (3)	17.73 (4)
433.5	0.638	19.9 (1)	19.40 [9]	0.948 (1)	11.54 (7)	7.42 (6)	12.73 (6)

Table 4: continued.

T	x_1	p	p^{exp}	y_1	ρ'	ρ''	Δh_v
K	mol/mol	MPa	MPa	mol/mol	mol/l	mol/l	kJ/mol
Cyclohexane (1) + Cyclohexanone (2)							
323.15	0.0	0.0018(1)	0.002 [2]	0	9.220(1)	0.0006(1)	45.979(8)
323.15	0.096	0.0111(8)	0.010 [10]	0.84 (2)	9.181(1)	0.0041(3)	44.174(6)
323.15	0.275	0.0201(8)	0.019 [10]	0.926 (6)	9.109(1)	0.0075(3)	41.041(7)
323.15	0.565	0.0283(7)	0.028 [10]	0.956 (2)	8.999(1)	0.0107(3)	36.564(7)
323.15	0.892	0.0343(7)	0.034 [10]	0.984 (1)	8.904(1)	0.0129(3)	32.622(5)
323.15	1.0	0.0370(7)	0.036 [1]	1	8.895(1)	0.0140(1)	31.691(6)
348.15	0.0	0.0058(3)	0.007 [2]	0	8.995(1)	0.0020(1)	44.456(9)
348.15	0.141	0.031 (1)	0.030 [10]	0.832 (9)	8.932(1)	0.0110(1)	41.874(7)
348.15	0.249	0.045 (1)	0.044 [10]	0.891 (5)	8.882(1)	0.0157(1)	40.007(7)
348.15	0.442	0.057 (1)	0.058 [10]	0.927 (3)	8.791(1)	0.0202(4)	36.937(7)
348.15	0.792	0.075 (1)	0.075 [10]	0.964 (1)	8.656(1)	0.0266(4)	32.381(6)
348.15	1.0	0.0863(9)	0.085 [1]	1	8.608(2)	0.0307(3)	30.418(7)

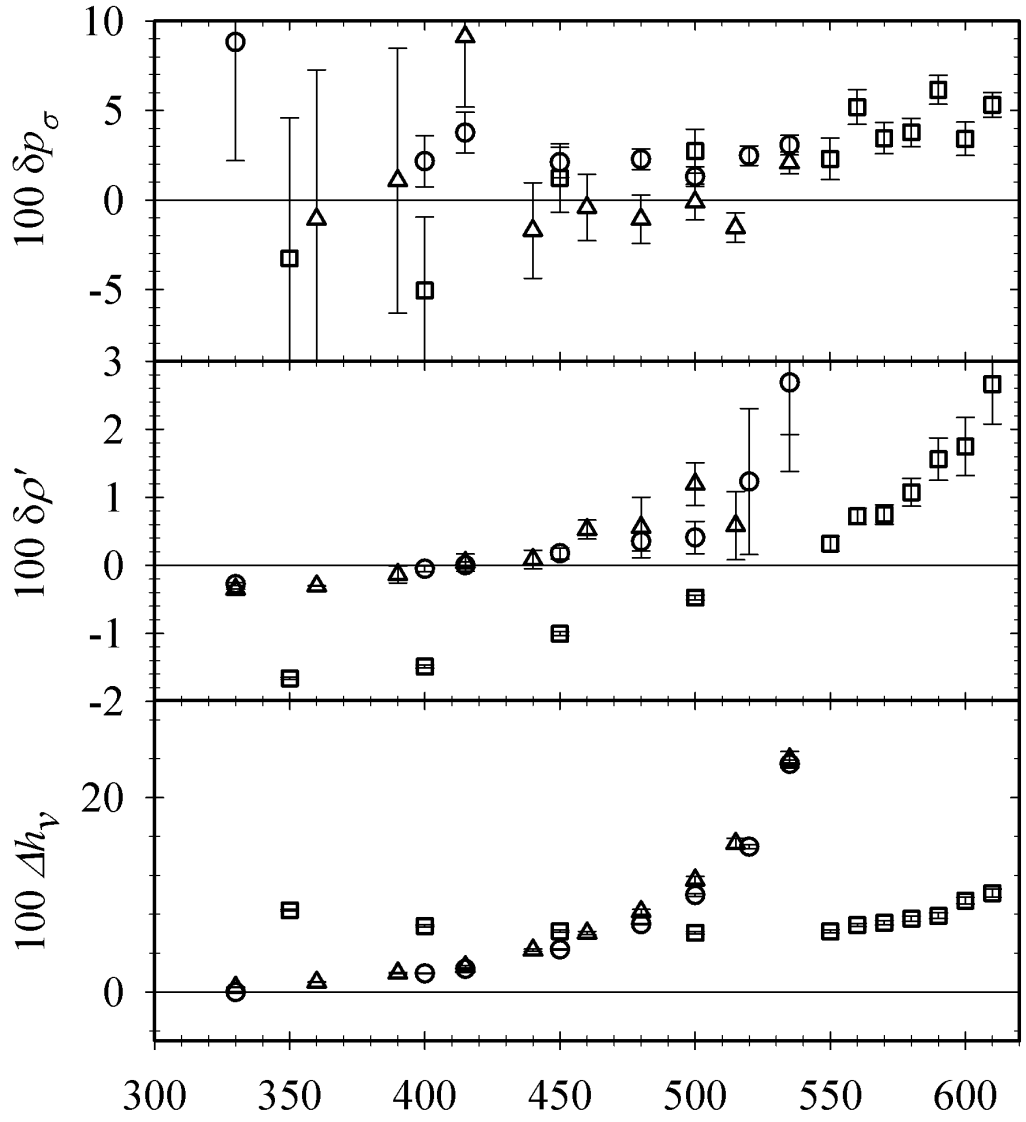

Figure 1: Relative deviations of vapor-liquid equilibrium properties between simulation data and a reference EOS [1] or a DIPPR correlation [2] ($\delta z = (z_{\mathrm{sim}} - z_{\mathrm{EOS}})/z_{\mathrm{EOS}}$): ○ cyclohexane, this work; □ cyclohexanone, this work; △ cyclohexane model by Eckl et al. [3]. From top to bottom: vapor pressure, saturated liquid density and enthalpy of vaporization.

References

[1] S. G. Penoncello, A. R. H. Goodwin, R. T. Jacobsen, Int. J. Thermophys. 16 (1995) 519–531.

[2] R. L. Rowley, W. V. Wilding, J. L. Oscarson, Y. Yang, N. A. Zundel, T. E. Daubert, R. P. Danner, DIPPR® Data Compilation of Pure Compound Properties, Design Institute for Physical Properties, AIChE, New York, 2006.

[3] B. Eckl, J. Vrabec, H. Hasse, J. Phys. Chem. B 112 (2008) 12710–12721.

[4] T. Merker, N. Franke, R. Gläser, T. Schleid, H. Hasse, J. Chem. Eng. Data 56 (2011) 2477–2481.

[5] M. C. Esmelindro, O. A. C. Antunes, E. Franceschi, G. R. Borges, M. L. Corazza, J. V. Oliveira, W. Linhares, C. Dariva, J. Chem. Eng. Data 53 (2008) 2050–2055.

[6] N. Nagarajan, R. L. J. Robinson, J. Chem. Eng. Data 32 (1987) 369–371.

[7] S. K. Shibata, S. I. Sandler, J. Chem. Eng. Data 34 (1989) 419–424.

[8] Y. Feng, W. Hu, Y. Hou, Gaoxiao Huaxue Gongcheng Xuebao 6 (1992) 19–24.

[9] S. Laugier, D. Richon, J. Chem. Eng. Data 42 (1997) 155–159.

[10] T. Boublik, B. C. Y. Lu, J. Chem. Eng. Data 22 (1977) 331–333.